Available online at www.sciencedirect.com
ScienceDirect
Journal of Nuclear Materials 367–370 (2007) 823–828
journal of nuclear materials
www.elsevier.com/locate/jnucmat

Impurity behavior in V–4Cr–4Ti–Y alloys produced by levitation melting

Takuya Nagasaka [a,*], Takeo Muroga [a], Takeshi Hino [b], Manabu Satou [b], Katsunori Abe [b], Toshinori Chuto [b,1], Tomohito Iikubo [c]

[a] National Institute for Fusion Science, Oroshi 322-6, Toki, Gifu 509-5292, Japan
[b] Graduate School of Engineering, Tohoku University, Sendai 980-8579, Japan
[c] Daido Bunseki Research, Inc., Nagoya 457-8545, Japan

Abstract

An alloy of V–4Cr–4Ti–0.15Y was fabricated by 15 kg-scale magnetic levitation melting. The oxygen level was successfully reduced to 108 wppm by slag-out of Y_2O_3 formation on the surface of the melted ingot. Y_2O_3 was identified as a new type of precipitate, in addition to Ti–O type and Ti–N type precipitates common in V–4Cr–4Ti alloys. Y_2O_3 formation is thought to reduce the amount of oxygen in solid solution state and in unstable Ti–O type precipitates. Based on the behavior of the O impurity, optimum fabrication processes for V–4Cr–4Ti–0.15Y alloy were suggested.

1. Introduction

It has been shown that reduction of the oxygen level and control of Ti–C, N, O precipitate distributions are critical to various properties of V–4Cr–4Ti alloys [1–4]. Yttrium (Y) addition is well known to be effective for reduction of the oxygen level by slag formation on the melting ingot surface [5]. Because of the slag layer, the conventional large-scale melting processes, such as continuous arc-melting and electron beam melting, cannot be used for fabricating Y containing alloys. The present authors have developed magnetic levitation melting as a new process for producing high purity V–4Cr–4Ti–Y alloy [6]. Previous studies with 2 kg-scale melting showed that the oxygen concentration was decreased with increasing Y concentration, while workability and impact properties were degraded. The addition of 0.15 wt% Y has been selected for larger scale melting from a trade-off between oxygen level and impact properties [7]. In the present paper, the V–4Cr–4Ti–0.15Y alloy was fabricated by 15 kg-scale levitation melting. The Y effect on oxygen behavior in the melting and breakdown processes were investigated and optimum fabrication processes are discussed.

2. Experimental procedure

The starting pure V, Cr and Ti were the same grades as used for the reference high purity

* Corresponding author. Tel.: +81 572 58 2252; fax: +81 572 58 2676.
E-mail address: nagasaka@nifs.ac.jp (T. Nagasaka).
[1] Present address: Japan Atomic Energy Agency, Ibaraki 319-1195, Japan.

0022-3115/$ - see front matter © 2007 Published by Elsevier B.V.
doi:10.1016/j.jnucmat.2007.03.076

V–4Cr–4Ti alloy, NIFS-HEAT (NH) [8]. C, N and O impurity levels in the starting Y were 210, 380 and 823 wppm, respectively. A 15 kg V–4Cr–4Ti–0.15Y ingot was melted under flowing Ar gas (containing O_2: 0.62 ppm, N_2: 0.59 ppm) in a levitation furnace with induction heating of 450 kW and 15 kHz for about 30 min. The resulting ingot (156 mm diameter × 166 mm) was cut into two pieces to investigate the homogeneity of constituent elements and the macrostructure in the vertical cross section using X-ray diffraction analysis (XRD), scanning electron microscopy (SEM) and energy dispersive X-ray analysis (SEM–EDX). As shown in Fig. 1, the ingot contained an equiaxed crystal zone and a cylindrical (elongated) crystal zone. Small blocks $8 \times 8 \times 37$ mm were cut from the equiaxed zone, and processed by working and recrystallization treatments. One block was cold rolled to 1 mm-thick sheet (88% in reduction of thickness) and then recrystallized at 873–1373 K for 1 h. The other block was annealed at 1273 K for 1 h before the same cold rolling and recrystallization anneals. The sheet without annealing at 1273 K is indicated as V–4Cr–4Ti–0.15Y, and the one with the annealing is V–4Cr–4Ti–0.15Y*. After the 1373 K annealing, some specimens were heated again to 973 K for 1 h. This treatment cycle is called a 're-precipitation treatment', where fine Ti–C–O type precipitation

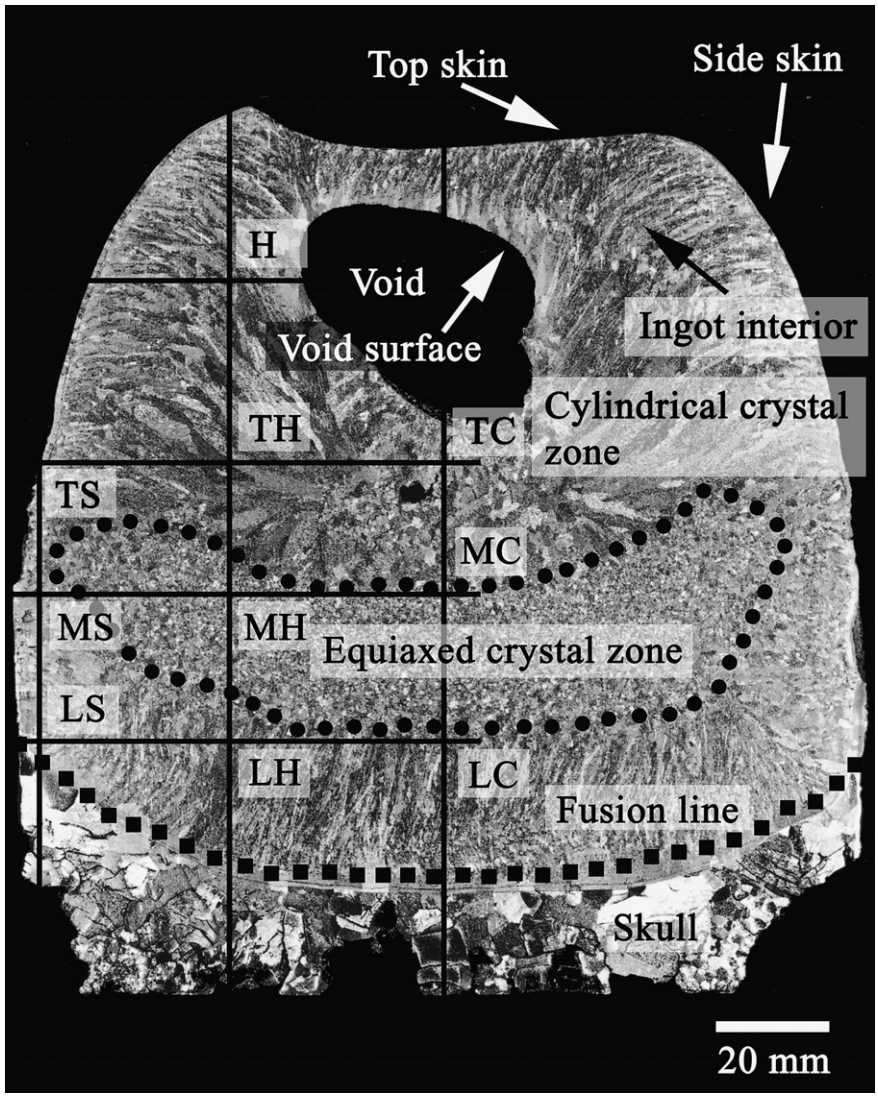

Fig. 1. Cross section of the V–4Cr–4Ti–0.15Y ingot fabricated by levitation melting.

and significant hardening occurred in NH [9]. Recovery of the hardness and the recrystallization processes were analyzed using hardness measurements with a load of 500 g for 30 s, SEM, transmission electron microscopy (TEM) and TEM–EDX.

3. Results

Fig. 1 shows a macrostructure of the cross section of the V–4Cr–4Ti–0.15Y ingot. The cross section shows four zones: (1) the equiaxed crystal zone enclosed by a doted line, (2) the cylindrical crystal zone outside of the equiaxed zone, (3) voids observed near the top of the ingot and (4) unalloyed skull separated by a dashed fusion line at the bottom. The alloyed zones were chemically analyzed at the 10 cross points of the black lines. Table 1 lists the results of the chemical analysis. Chemical composition was very homogeneous except for Cr and Ti concentrations at the LS point, which is close to the fusion line. No differences of compositions were detected between the equiaxed and cylindrical crystal zones. Fig. 2 shows the detailed chemical analysis around the fusion line determined by SEM–EDX. Concentrations of Cr and Ti reached constant values within 1 mm of the fusion line. Fig. 3 shows XRD spectrum at the locations identified by arrows in Fig. 1. The Y_2O_3 compound was clearly detected at the top and side skin of the ingot. A weak peak from Y_2O_3 (circled) was also detected at the inner surface of the void.

During cold rolling of the as-melted alloy, visible cracks were observed at both the ears and surfaces of the sheet, which is called V–4Cr–4Ti–0.15Y.

Table 1
Chemical composition at several locations in the V–4Cr–4Ti–0.15Y ingot

Position[a]	Cr (wt%)	Ti (wt%)	Y (wt%)	C (wppm)	N (wppm)	O (wppm)
H	4.54	4.70	0.10	110	130	80
TC	4.54	4.78	0.10	130	140	100
TH	4.55	4.76	0.10	120	110	110
TS	4.57	4.71	0.10	90	130	130
MC	4.51	4.59	0.09	120	130	110
MH	4.51	4.59	0.09	110	130	110
MS	4.50	4.59	0.09	110	120	120
LC	4.50	4.57	0.09	110	120	110
LH	4.50	4.56	0.09	120	150	100
LS	2.31	1.71	0.08	90	120	110

[a] Position shown in Fig. 1.

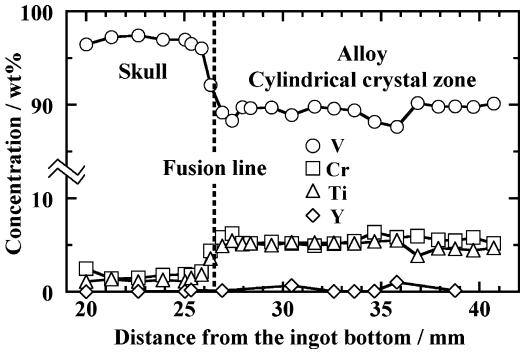

Fig. 2. Chemical composition measured by SEM–EDX around the fusion line indicated in Fig. 1.

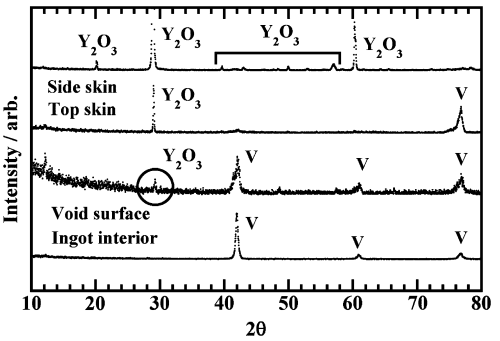

Fig. 3. XRD spectrum at locations shown by arrows in Fig. 1.

The conditioning anneal at 1273 K for 1 h of the as-melted alloy was very effective in improving workability, so that a fine sheet with no cracking (called V–4Cr–4Ti–0.15Y*) was obtained. Most analyses were done on the V–4Cr–4Ti–0.15Y*. Fig. 4 shows hardness recovery for final annealing (873–1373 K for 1 h) and the precipitation treatment (1373 K for 1 h + 973 K for 1 h) of the cold-rolled sheet. Fig. 4 also plots previous data for NH1 [9]. Hardness of as-rolled Y containing alloys was much lower than that of NH1. For 1073–1273 K annealing, the hardness of Y containing alloy was similar to NH1, where minimum hardness was found at 1223 K. At 1373 K annealing, hardness of NH1 was higher than that at 1223 K, whereas Y containing alloy indicated lower hardness. Especially following the 973 K annealing (precipitation treatment), NH1 resulted in large hardening. In contrast, Y containing alloys exhibited little or no hardening. SEM observations indicated that full, isotropic recrystallization occurred at 1173 K or higher temperatures. Grain

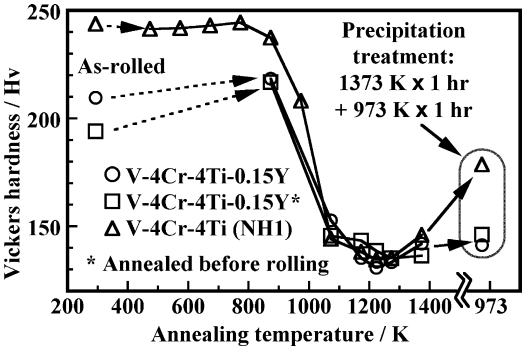

Fig. 4. Recovery of hardness by final annealing (873–1373 K) and precipitation treatment (1373 K then 973 K) in the rolled sheet with and without intermediate annealing before cold rolling.

growth for annealing at 1173–1373 K was examined. For example, grain size of V–4Cr–4Ti–0.15Y and V–4Cr–4Ti–0.15Y* was 23 and 17 μm, respectively, after annealing at 1223 K, while it was 36 and 30 μm at 1273 K, respectively. Grain size of the Y containing alloys below 1223 K was 16–23 μm, whereas it was 30–44 μm above 1273 K.

Fig. 5 shows the TEM microstructures, comparing with NH1. Three different size classes of precipitates were observed in V–4Cr–4Ti–0.15Y, while NH1 contained only 2 types. The number density of the precipitates varied between observed areas. Small precipitates, less than 100 nm in size with plate or bar shape are shown in Fig. 5(b), while medium ones ranged from 100 nm to 1 μm, and appeared as sphere or elongated shapes are seen in Fig. 5(a). Large precipitates, 1–10 μm in size and with irregular shape are shown in Fig. 5(c). The TEM microstructures in the temperature range, 1173–1373 K were similar. In NH1 Fig. 5(d), only small and medium size precipitates were observed. The major differences between NH1 and Y containing alloys were a lower number density of the small precipitates and appearance of the large precipitates in V–4Cr–4Ti–0.15Y*. After the precipitation treatment, fine and homogeneously-distributed precipitates were observed. The precipitate size in V–4Cr–4Ti–0.15Y* (Fig. 5(e)) was larger, but the number density was over one order smaller than in NH1 (Fig. 5(f)). Fig. 6 shows TEM–EDX spectrum for the large and medium size precipitates in V–4Cr–4Ti-0.15*. Yttrium was only identified in large precipitates, while medium precipitate indicated a Ti-rich composition. In order to investigate the stability of the large precipitates, sections of the

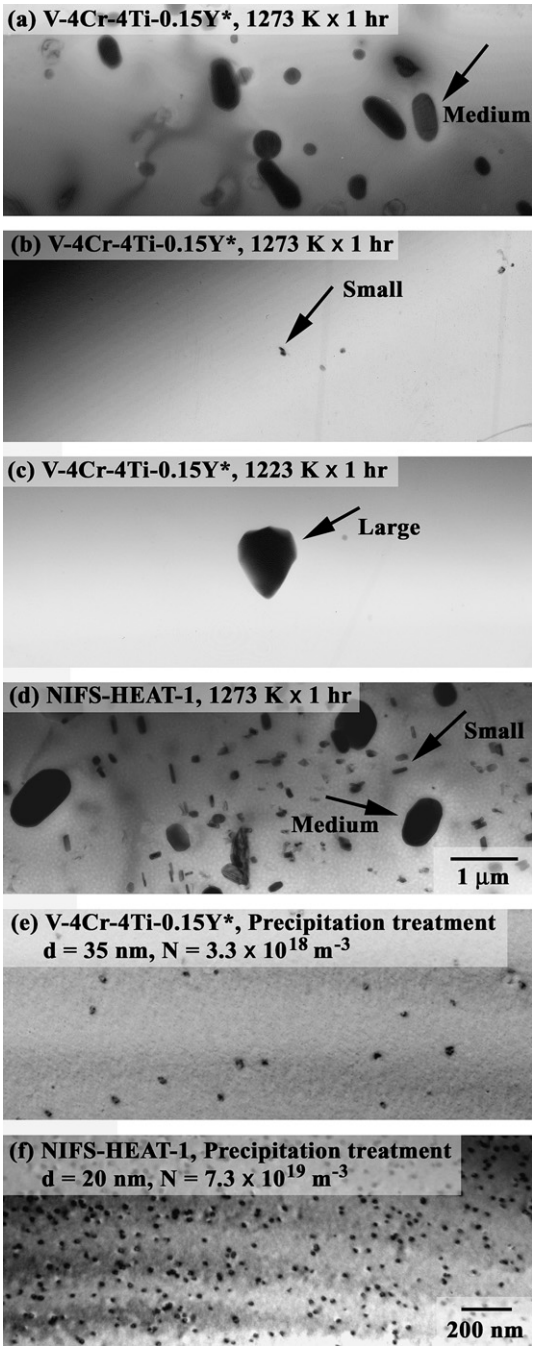

Fig. 5. TEM microstructures after final annealing at 1223 K or 1273 K, and precipitation treatment (1373 K × 1 h + 973 K × 1 h). Precipitates observed in (a)–(d) were categorized into 3 groups by size and shape. For (e) and (f) conditions, average size, d, and number density, N, of the precipitates are shown.

as-melted ingot were heat treated at 1273 K and 1423 K, and analyzed by SEM. The large precipitates were already observed in as-melted ingot,

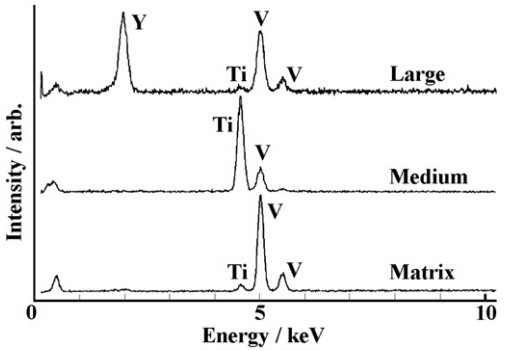

Fig. 6. TEM–EDX spectrum for two classes of precipitates and the matrix in V–4Cr–4Ti–0.15Y*.

and underwent no change in morphology during the 1273 K or 1423 K annealing.

4. Discussion

4.1. Impurity behavior during melting

The results in Table 1 and Fig. 2 show that good homogeneity in the 15 kg-scale ingot of V–4Cr–4Ti–0.15Y alloy was demonstrated. Good mixing was achieved in the melt, where Y_2O_3 formed was transferred to the surface and produced a slag layer that protected against impurity contamination from the atmosphere. The average C/N/O concentrations were 113/129/108 wppm, respectively. The initial Y addition was 0.15 wt%, however the residual Y was 0.094 wt% on average. The difference, 0.056 wt%, was consumed in oxygen protection and removal in the slag-out mechanism. The remaining Y, 0.094 wt%, can consume O to 255 wppm, which is more than enough to trap all O as Y_2O_3 according to the average O concentration of 108 wppm. Electrolytic extraction analysis is planed in future to separate the amount of Y_2O_3 produced inside the ingot, and Y in solid solution.

The oxygen level was lower than in NH1 (181 wppm) and NH2 (122 and 148 wppm) [8], and the C and N levels were larger that in NH1 and NH2 (C: 50–69 wppm, N: 96–122 wppm). Neither YC nor YN compounds were detected at the ingot skin as shown in Fig. 3. C and N from the atmosphere are believed to diffuse in the Y_2O_3 slag and to reach the melt without slag formation. This small amount of contamination is thought to have little significant effect on mechanical properties, however minimization of melting time and good circulation of the melt can further reduce C and N contamination.

4.2. Oxygen behavior in breakdown process

The morphology of the small and medium size precipitates observed in Fig. 5(a) and (b), and the results of TEM–EDX analysis in Fig. 6, show they are the Ti–C, N, O precipitates common in V–4Cr–4Ti alloys [10]. The number density of the medium sized precipitates increased with increasing O and especially with increasing nitrogen levels. Since the contribution of nitrogen was much larger than oxygen, the main compound of the medium precipitates is believed to be Ti–N [9]. The number density of the small precipitates increased with increasing O addition, therefore the main compound should be Ti–O [9]. As in NH1 and NH2, the small Ti–O precipitates likely disappeared after 1373 K annealing in V–4Cr–4Ti–0.15Y*. Dissolution of the small Ti–O precipitates would release O into solution. At 973 K, the dissolved oxygen recombined to form the fine, homogeneously distributed precipitates in NH1, which lead to significant hardening indicated in Fig. 4 (Precipitation treatment). In V–4Cr–4Ti–0.15Y*, however, the number density in the re-precipitation was much smaller than in NH1, therefore hardening was lower after the precipitation hardening. In Y containing alloys, it was thought that O was trapped in the large and stable Y_2O_3. This trapping decreases the partition of O to the small and unstable Ti–O precipitates. The distribution of the Y_2O_3 inclusions was too inhomogeneous to allow quantitative analysis by TEM. However, SEM analysis showed that the size and number density was stable during heat treatment at 1273 K and 1423 K, which is in the hot working temperature range.

Assuming that (1) O contents in the re-precipitated Ti–O are the same in V–4Cr–4Ti–0.15Y* and NH1, and (2) the precipitates are disk with diameter, d, as indicated in Fig. 5(e) and (f), and with the same thickness, t, then reduction of O amount contributing to the unstable Ti–O precipitates can be estimated by comparing the total volume of the precipitates.

$$\frac{(N\pi(d/2)^2 t)_{\mathrm{V-4Cr-4Ti-0.15Y*}}}{(N\pi(d/2)^2 t)_{\mathrm{NH1}}} = \frac{3.3\times10^{18}\ \mathrm{m^{-3}}\times(35\ \mathrm{nm})^2}{7.3\times10^{19}\ \mathrm{m^{-3}}\times(20\ \mathrm{nm})^2} = 14\%. \quad (1)$$

In V–4Cr–4Ti–0.15Y*, only 14% as much O is trapped in the small Ti–O precipitates as in the NH1. Most O is trapped in the Y_2O_3 formed on melting.

4.3. Optimization of the fabrication processes

For melting conditions in the present study, O was successfully removed by slag-out with good mixing, and the resulting ingot was very homogeneous in composition. However, as mentioned above, C and N contamination maybe reduced further, if melting time is minimized with continuous circulation.

A relatively large void in the top of the ingot and Y_2O_3 on the void inner surface were detected as shown in Figs. 1 and 3 (circled). Since the Y_2O_3 slag layer at the void surface can be a large inclusion, degrading some mechanical properties, this void should be removed before the breakdown process. The void was produced by shrinkage at solidification. The void size can be reduced by a hot topping technique which is common in steel making, and by a reduced cooling rate, so that yield would be improved.

Hot working should be conducted near 1273 K, where workability was improved. After hot working, cold rolling can be used to at least 88% in reduction of thickness without any intermediate annealing. For final annealing, 1223 K was determined to be the optimum temperature, because hardness showed a minimum and interstitial O is expected to be very low due to trapping in Y_2O_3 and Ti–O precipitates; moreover about 20 μm in grain size was not different significantly from that in NH1, and with this grain size good mechanical and irradiation properties have already been demonstrated [2,11].

5. Conclusions

(1) V–4Cr–4Ti–0.15Y alloy was fabricated by 15 kg-scale levitation melting. Oxygen level was successfully reduced to 108 wppm, which is lower than the reference V alloy NIFS-HEATs (>150 wppm). Y_2O_3 slag was formed at the surface of the melted ingot. The Y addition was effective to slag-out oxygen and protection from oxygen contamination during melting.

(2) In addition to Ti–O and Ti–N type precipitates common in V–4Cr–4Ti alloys, Y_2O_3 type precipitates (inclusions) were observed. Y_2O_3 formation is thought to reduce the amount of O in solid solution state and in unstable Ti–O type precipitates. Since oxygen is believed to interact with irradiation defects, and O in solution is much lower in Y containing alloys, neutron irradiation hardening and embrittlement could be improved for the Y containing alloys.

(3) The following breakdown process was suggested.
   – Trim the ingot to remove the surface slag layer and the void.
   – Hot work at a temperature of 1273 K.
   – Cold roll without intermediate annealing up to 88% in reduction of thickness.
   – Final anneal at 1223 K for 1 h.

Acknowledgements

This study was supported by National Institute for Fusion Science budget code NIFS05UCFF005. Authors are grateful to Mr Oku and Miss Sekine for supports in experiments.

References

[1] M. Satou, T. Chuto, K. Abe, J. Nucl. Mater. 283–287 (2000) 367.
[2] T. Nagasaka, N.J. Heo, T. Muroga, A. Nishimura, H. Watanabe, M. Narui, K. Shinozaki, J. Nucl. Mater. 329–333 (2004) 1539.
[3] T. Nagasaka, N.J. Heo, T. Muroga, M. Imamura, Fusion Eng. Des. 61&62 (2002) 757.
[4] T. Nagasaka, M.L. Grossbeck, T. Muroga, J.F. King, Fusion Technol. 39 (2001) 664.
[5] M. Satou, K. Abe, H. Kayano, J. Nucl. Mater. 179–181 (1991) 757.
[6] T. Chuto, T. Nagasaka, T. Muroga, M. Satou, K. Abe, T. Shibayama, S. Tomiyama, M. Sakata, J. Inst. Mater. 64 (2000) 743.
[7] T. Chuto, M. Satou, A. Hasegawa, K. Abe, T. Muroga, N. Yamamoto, J. Nucl. Mater. 326 (2004) 1.
[8] T. Nagasaka, T. Muroga, Y.C. Wu, Z.Y. Xu, M. Imamura, J. Plasma Fus. Res. Ser. 5 (2002) 545.
[9] N.J. Heo, T. Nagasaka, T. Muroga, H. Matsui, J. Nucl. Mater. 307–311 (2002) 620.
[10] N.J. Heo, T. Nagasaka, T. Muroga, J. Nucl. Mater. 325 (2004) 53.
[11] T. Nagasaka, T. Muroga, H. Watanabe, K. Yamasaki, N.J. Heo, K. Shinozaki, M. Narui, Mater. Trans. 46 (2005) 498.